

Reading, writing and squeezing the entangled states of two nanomechanical resonators coupled to a SQUID

Guy Z. Cohen* and Massimiliano Di Ventra†

Department of Physics, University of California, San Diego, La Jolla, California 92093-0319

We study a system of two nanomechanical resonators embedded in a dc SQUID. We show that the inductively-coupled resonators can be treated as two entangled quantum memory elements with states that can be read from, or written on by employing the SQUID as a displacement detector or switching additional external magnetic fields, respectively. We present a scheme to squeeze the even mode of the state of the resonators and consequently reduce the noise in the measurement of the magnetic flux threading the SQUID. We finally analyze the effect of dissipation on the squeezing using the quantum master equation, and show the qualitatively different behavior for the weak and strong damping regimes. Our predictions can be tested using current experimental capabilities.

I. INTRODUCTION

In recent years nanoelectromechanical systems^{1,2} (NEMs), nanoscale mechanical oscillators coupled to electronic devices of comparable dimensions, have attracted substantial research effort. A major motivation for this effort is the ability to observe quantum behavior in a macroscopic system under realizable experimental conditions^{3,4}. Indeed, NEMs today can be fabricated with vibrational mode frequencies of 1 MHz-10 GHz and quality factors in the range of $10^3 - 10^5$, allowing the quantum regime to be reached at milli-Kelvin temperatures for high frequency oscillators^{5,6}. Possible quantum effects in NEMs under such conditions include quantized energy levels, superposition of states, entanglement and squeezing⁷⁻⁹. In addition, NEMs are applied to high-sensitive detection of mass¹⁰⁻¹², force¹³ and displacement¹⁴, electrometers¹⁵, and also to classical memory elements^{16,17}.

Observing or changing the state of NEMs requires some type of transducer which couples to them. Optical coupling¹⁸ can be performed, e.g., by a microwave cavity¹⁹, but is difficult to integrate in circuits and suffers from the diffraction limit and heating of the NEMS. Non-optical coupling methods are therefore more common in experiments today. With magnetomotive coupling²⁰, the magnetic force on a thin metallic layer on the NEMS is measured. Capacitive coupling can take many forms, one of which uses a normal or superconducting single electron transistor (SET)^{8,21}. The NEMS changes the island charging energy in the SET and hence the tunneling rates, which can be read electronically. Other forms of capacitive coupling use Cooper pair boxes^{22,23}, flux qubits²⁴, quantum point contacts²⁵ and quantum dots²⁶.

An inductive coupling scheme with a potential for displacement precision greater than the standard quantum limit is obtained by integrating a doubly clamped micron-scale beam within a superconducting quantum interference device (SQUID). In a dc SQUID the motion of the resonator changes the area of the SQUID loop and hence the magnetic flux and the current through it, which is then measured. This system was only recently

implemented^{27,28}. A more sophisticated design, where the dc SQUID, and hence the resonator, is coupled to a charge qubit, was also proposed⁹. For an rf SQUID it was found²⁹ that the change in the magnetic flux due to the motion of the beam affects the visibility of Rabi oscillations in the SQUID levels. The detection of discrete Fock states in a resonator integrated with an rf SQUID was suggested in another work³⁰.

Squeezed states, originally introduced in quantum optics³¹, are defined as minimum-uncertainty states with less noise in one field quadrature than a coherent state³². Several methods to generate squeezing in NEMs were suggested. Coupling to a charge qubit^{7,9} as means of generating squeezing was proposed, while another work described squeezing by periodic position measurement with a weakly-coupled detector⁸. Squeezing in nanoresonators can be applied to decrease the noise in force or displacement measurements to below the standard quantum limit, greatly improving the sensitivity of the device^{7,33}.

In this work, we present a scheme to create quantum entanglement and squeezing in two nanoresonators integrated in a dc SQUID. A previous study³⁴ analyzed a similar system but introduced many approximations that are difficult to implement experimentally, whereas our present study is closer to an experimentally realizable system. For instance, we do not overlook the generally non-negligible self-inductance of the SQUID as done in previous work³⁴, and we assume mega-Hertz frequency nanomechanical oscillators rather than giga-Hertz frequency resonators, which are difficult to integrate with a SQUID. Lastly, we do not require the SQUID to be prepared in a high- $|\alpha|$ coherent state in order to have squeezing, as the previous study does³⁴, and require instead a thermal equilibrium state, which is easier to accomplish. Finally, we consider different aspects of the system and draw conclusions, e.g., on the reading and writing processes, that were not advanced in previous literature.

The paper is organized as follows. In Sec. II we present the system model and its classical Lagrangian and Hamiltonian formulations. We then proceed to quantize the Hamiltonian for the non-dissipative case and derive the effective Hamiltonian. Next, in Sec. III we treat the

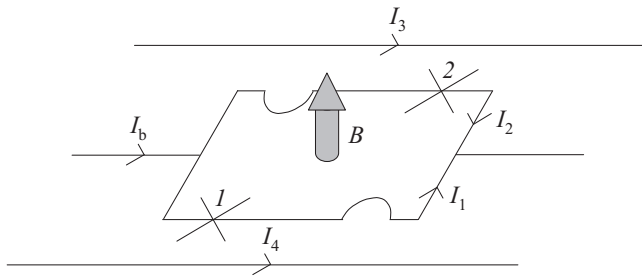


FIG. 1. Schematic of the device we study: Two nanomechanical beams oscillating in plane are embedded in a dc SQUID with area A when beams are at rest. Uniform magnetic field B threads the SQUID, and bias current I_b is assumed. The two identical Josephson junctions on the SQUID have phase drops γ_i ($i = 1, 2$). The currents I_3 and I_4 create additional magnetic fields B_1 and B_2 at the resonators.

system as a quantum memory and explain how one can read its quantum state or write on it. In Sec. IV we put forward a scheme for generating quadrature-squeezed states of the nanomechanical beams when dissipation is neglected, whereas in Sec. V we use a quantum master equation approach to test the range of validity of our results in the presence of dissipation. Lastly, we discuss our results and present the conclusions in Sec. VI.

II. SYSTEM MODEL AND HAMILTONIAN

Our system consists of a dc SQUID, shown schematically in Fig. 1, in which each arm includes a Josephson junction and an integrated doubly clamped beam of length l_i and mass m_i that can oscillate mechanically in the plane of the SQUID with an angular frequency $\tilde{\omega}_i$ ($i = 1, 2$). The notation we use is similar to the one in Ref. 35. A uniform magnetic field B is applied perpendicularly to the plane of the loop, and a dc bias current I_b flows through it after splitting to I_1 and I_2 in the lower and upper arms, respectively. Two current-carrying wires with currents I_3 and I_4 create additional magnetic fields B_1 and B_2 at the positions of the first and second beams, respectively. The beam amplitudes are much smaller than the beam-wire distance, allowing these fields to be approximated as being spatially uniform. For simplicity, the two Josephson junctions on the SQUID arms are taken to be identical and their gauge-invariant phase changes are denoted by γ_i . The critical current and shunting capacitance of each junction are taken as I_c and C , respectively, and are used to define the characteristic junction energy scales: the Josephson energy $E_J = \hbar I_c / 2e$ and the charging energy $E_C = e^2 / 2C$. The plasma frequency $\omega_{pl} = \sqrt{2E_J E_C} / \hbar$ sets the typical time scale for the SQUID dynamics.

The area of the SQUID loop depends on the center of mass positions of the nanomechanical resonators, denoted by x_i and defined as zero when the beam is at rest,

and positive when it is inside the loop. Since the superconducting order parameter is single valued, we must have

$$\gamma_1 - \gamma_2 - \frac{2\pi\Phi}{\Phi_0} = 2\pi p, \quad (1)$$

$$\Phi = BA - \sum_i (B + B_i) l_i x_i + L(I_1 - I_2)/2, \quad (2)$$

where p is an integer, Φ is the total magnetic flux threading the loop, A is the loop area when the beams are at rest, $\Phi_0 = h/2e$ is the flux quantum, L is the self-inductance of the loop, and I_i is the current in its i th arm. The first term in Eq. (2) comes from the external magnetic field and the second, responsible for the coupling of the mechanical and magnetic degrees of freedom, from the oscillation of the beams. The difference between $l_i x_i$ and the actual area enclosed by the i th beam is negligible, being of third order in the ratio of the beam amplitude to its length. Lastly, the third term originates from the magnetic flux induced by the circulating current in the SQUID.

The kinetic and potential energies of the system are functions of four dimensionless variables defined by $\gamma = (\gamma_1 + \gamma_2)/2$, $\phi = \Phi/\Phi_0$ and $\xi_i = (B + B_i) l_i x_i / \Phi_0$. They are

$$T = \sum_i \left(\frac{\hbar^2}{4E_C} \frac{1}{\Omega_i^2} \frac{1}{\mathcal{A}_i^2} \dot{\xi}_i^2 \right) + \frac{\hbar^2}{2E_C} \dot{\gamma}^2 + \frac{\pi^2 \hbar^2}{2E_C} \dot{\phi}^2, \quad (3)$$

$$U = E_J [-2 \cos \gamma \cos(\pi\phi) - \frac{I_b}{I_c} \gamma + \sum_i ((-1)^i \pi \frac{I_b}{I_c} \xi_i + \frac{\xi_i^2}{2\mathcal{A}_i^2}) + \frac{2\pi}{\beta_L} (\phi - \xi_1 - \xi_2 - \phi_e)^2], \quad (4)$$

where mechanical dissipation was assumed to be negligible, and where we define the screening parameter $\beta_L = 2LI_c/\Phi_0$ and external flux $\phi_e = BA$ for the SQUID, while the dimensionless magnetic field

$$\mathcal{A}_i = \sqrt{\frac{E_J}{m_i}} \frac{(B + B_i) l_i}{\tilde{\omega}_i \Phi_0} \quad (5)$$

and oscillation frequencies $\Omega_i = \tilde{\omega}_i / \omega_{pl}$ are defined for each of the beams. The first term in Eq. (3) corresponds to the kinetic energy of the beams, while the second and third terms to the capacitive energy of the junctions. The first term in Eq. (4) relates to the Josephson energy, while the second term is the washboard potential term³⁶. The third term corresponds to the Lorentz force on the beams in the classical equations of motion (EOMs), and the fourth term to the beams' elastic potential, taken to be harmonic, as nonlinear terms are negligible at the amplitudes concerned³⁷. Lastly, the fifth term corresponds to the inductive energy of the SQUID.

The classical EOMs for the four variables γ, ϕ, ξ_1 and ξ_2 are the Euler-Lagrange equations for the system Lagrangian $\mathcal{L} = T - U$. Before writing the Hamiltonian, we expand the potential in series about a minimum $(\bar{\phi}, \bar{\gamma}, \bar{\xi}_1, \bar{\xi}_2)$, around which the system oscillates. Under current experimental conditions^{27,28} such a minimum exists, as the Hessian matrix for U there, proportional to

the one in Eq. 8, is positive definite. The well containing the minimum can accommodate ~ 20 states in γ and ~ 900 in ϕ . If we take these two parameters to be “frozen” at their respective ground states, as we will later assume, we find the well to be infinitely deep for the ξ_i parameters. This assumption also allows us to neglect in the series expansion of U terms higher than quadratic ones in $\phi - \bar{\phi}$ and $\gamma - \bar{\gamma}$. With these approximations in mind the Hamiltonian H reads

$$H = T + U = \sum_i \frac{E_C}{2\hbar^2} p_i^2 + \sum_{i,j} E_J V_{ij} q_i q_j, \quad (6)$$

where the coordinates q_i are given by

$$q_1 = \gamma - \bar{\gamma}, \quad q_2 = \pi(\phi - \bar{\phi}), \quad q_{2+j} = \frac{1}{\sqrt{2}\Omega_j \mathcal{A}_j} (\xi_j - \bar{\xi}_j) \quad (7)$$

($j = 1, 2$), and the canonically conjugate momenta p_i are $p_i = (\hbar^2/E_C)\dot{q}_i$. In addition,

$$V = \begin{pmatrix} r & -s & 0 & 0 \\ -s & r + \frac{2}{\pi\beta_L} & -\frac{2\sqrt{2}\Omega_1 \mathcal{A}_1}{\beta_L} & -\frac{2\sqrt{2}\Omega_2 \mathcal{A}_2}{\beta_L} \\ 0 & -\frac{2\sqrt{2}\Omega_1 \mathcal{A}_1}{\beta_L} & \Omega_1^2(1 + \frac{4\pi\mathcal{A}_1^2}{\beta_L}) & \frac{4\pi\Omega_1 \mathcal{A}_1 \Omega_2 \mathcal{A}_2}{\beta_L} \\ 0 & -\frac{2\sqrt{2}\Omega_2 \mathcal{A}_2}{\beta_L} & \frac{4\pi\Omega_1 \mathcal{A}_1 \Omega_2 \mathcal{A}_2}{\beta_L} & \Omega_2^2(1 + \frac{4\pi\mathcal{A}_2^2}{\beta_L}) \end{pmatrix}, \quad (8)$$

where $r = \cos\bar{\gamma} \cos(\pi\bar{\phi})$ and $s = \sin\bar{\gamma} \sin(\pi\bar{\phi})$ were introduced. We see that the beam oscillations are coupled inductively via the V_{34} term. This coupling can be used to generate squeezed states in the beams as we will show below.

The Hamiltonian is quantized in the standard way by converting the coordinates q_i and their canonically conjugate momenta p_i to operators and postulating the canonical commutation relation $[\hat{q}_i, \hat{p}_j] = i\hbar\delta_{ij}$. In terms of creation and annihilation operators \hat{q}_i and \hat{p}_i are

$$\hat{q}_i = \frac{1}{2} \left(\frac{2E_C}{E_J V_{ii}} \right)^{1/4} (a_i^\dagger + a_i), \quad (9)$$

$$\hat{p}_i = i\hbar \left(\frac{E_J V_{ii}}{2E_C} \right)^{1/4} (a_i^\dagger - a_i), \quad (10)$$

and the quantized Hamiltonian is given by

$$H = \sum_i \hbar\omega_i (a_i^\dagger a_i + \frac{1}{2}) + \frac{1}{4} \hbar\omega_{pl} \sum_{i \neq j} \frac{\omega_{pl}}{\sqrt{\omega_i \omega_j}} V_{ij} (a_i + a_i^\dagger)(a_j + a_j^\dagger), \quad (11)$$

where $\omega_i = \omega_{pl} \sqrt{V_{ii}}$. We note the frequencies ω_3 and ω_4 are the same as the resonators frequencies, $\tilde{\omega}_1$ and

$\tilde{\omega}_2$, apart from each having a factor due to the magnetic field at the resonator. Thus we see that the Lagrangian classical memory variables ξ_1 and ξ_2 , in complete analogy with memory variables in electronic circuits³⁸, become memory quanta in the Hamiltonian.

Taking the same experimental conditions^{27,28} and tuning B to make r of order unity results in $\hbar\omega_1 \gg k_B T$ and $\hbar\omega_2 \gg k_B T$. Consequently, the first and second harmonic oscillators are “frozen” at their respective ground states. Moreover, since $\omega_1, \omega_2 \gg \omega_3, \omega_4$, exciting the nanomechanical oscillators will not budge them from their ground state. Removing constant terms, we are then left with the effective Hamiltonian

$$H = \hbar\omega_3 a_3^\dagger a_3 + \hbar\omega_4 a_4^\dagger a_4 + \tilde{V} (a_3 + a_3^\dagger)(a_4 + a_4^\dagger), \quad (12)$$

where the interaction coefficient reads

$$\tilde{V} = \frac{2\pi\hbar\sqrt{\tilde{\omega}_1 \tilde{\omega}_2} \mathcal{A}_1 \mathcal{A}_2}{\beta_L (1 + \frac{4\pi\mathcal{A}_1^2}{\beta_L})^{1/4} (1 + \frac{4\pi\mathcal{A}_2^2}{\beta_L})^{1/4}}. \quad (13)$$

III. READING AND WRITING QUANTUM INFORMATION

We now wish to employ this system to create entangled nanomechanical quantum memory that can be read from and written on. We assume the beams are cooled to a temperature low enough so as to reduce the equilibrium state to the ground state for each of the beams. This is possible today, e.g. by coupling to a superconducting microwave resonator³⁹, even if the environment of the beams, which includes the SQUID, has a higher temperature.

If the interaction term in Eq. (12) is small relative to the other two terms, perturbation theory gives first-order energy corrections in \tilde{V} only when $|\omega_3 - \omega_4| \ll \tilde{V}/\hbar$. Thus, we will henceforth assume the beams are identical. The Hamiltonian (12) is quadratic in the ladder operators and is thus amenable to an exact solution at all interaction strengths⁴⁰. This solution is found by moving to the differential representation and then diagonalizing the quadratic form of the potential by a canonical transformation to even and odd coordinates,

$$x_{e,o} = \frac{1}{\sqrt{2}}(x_1 \pm x_2), \quad p_{e,o} = \frac{1}{\sqrt{2}}(p_1 \pm p_2), \quad (14)$$

where x_i and p_i are the position and momentum coordinates of the i th beam.

Applying Eq. (14) on the ladder operators, we find

$$a_5 = \frac{1}{2\sqrt{2}} \left[\left(\sqrt{\frac{\omega_5}{\omega_3}} + \sqrt{\frac{\omega_3}{\omega_5}} \right) (a_3 + a_4) + \left(\sqrt{\frac{\omega_5}{\omega_3}} - \sqrt{\frac{\omega_3}{\omega_5}} \right) (a_3^\dagger + a_4^\dagger) \right], \quad (15)$$

$$a_6 = \frac{1}{2\sqrt{2}} \left[\left(\sqrt{\frac{\omega_6}{\omega_3}} + \sqrt{\frac{\omega_3}{\omega_6}} \right) (a_3 - a_4) + \left(\sqrt{\frac{\omega_6}{\omega_3}} - \sqrt{\frac{\omega_3}{\omega_6}} \right) (a_3^\dagger - a_4^\dagger) \right], \quad (16)$$

where a_5^\dagger corresponds to creation of an even mode quantum in which both beams oscillate in phase, and a_6^\dagger to creation of an odd mode quantum, where the beams oscillate in anti-phase. The even and odd oscillation frequencies are given by

$$\omega_{5,6} = \sqrt{\omega_3^2 \pm 2\tilde{V}\omega_3/\hbar}. \quad (17)$$

Using this transformation and omitting constant terms, the Hamiltonian (12) is reduced to

$$H = \hbar\omega_5 a_5^\dagger a_5 + \hbar\omega_6 a_6^\dagger a_6. \quad (18)$$

We see that the even mode is decoupled from the odd mode in this Hamiltonian, which is thus separable to an even and an odd part. The energy spectrum of this Hamiltonian is given by

$$E_{nm} = n\hbar\omega_5 + m\hbar\omega_6, \quad (19)$$

while the eigenstates are

$$|nm\rangle = \frac{1}{\sqrt{n!m!}} (a_5^\dagger)^n (a_6^\dagger)^m |00\rangle, \quad (20)$$

which, upon substitution of Eqs. (15) and (16), are seen to be highly entangled states of the two beams.

The quantum state of the system is read by measuring the magnetic flux threading through the SQUID, which is done by a current measurement in the standard way³⁶. The operator for this observable is

$$\hat{\Phi} = -(B + B_1)l_1x_1 - (B + B_2)l_2x_2, \quad (21)$$

where the constant term BA was omitted. With the assumption of $B_1 = B_2$, we have

$$\hat{\Phi} = -\sqrt{2}(B + B_1)l_1\lambda_3(a_5 + a_5^\dagger), \quad (22)$$

where the zero-point fluctuation, the resonator displacement uncertainty at the ground state, is defined as $\lambda_i = \sqrt{\hbar/2m_1\omega_{i+2}}$ with the definition extended also for $i = 3, 4$.

We thus see, as expected, that the measurement of the magnetic flux cannot detect the odd mode, since oscillations in this mode do not amount to a change in the area of the SQUID loop. We therefore set to read and write quantum information only in the n quantum number in the state $|nm\rangle$. Moreover, we note that for the eigenstates of the Hamiltonian we have $\langle\hat{\Phi}\rangle = 0$, implying that a better observable would be the standard deviation $\langle\Delta\hat{\Phi}\rangle$. This is indeed true, with the values of this observable on the eigenstates being

$$\langle\Delta\hat{\Phi}\rangle = \sqrt{2}(B + B_1)l_1\lambda_3\sqrt{1 + 2n}, \quad (23)$$

enabling us to measure the value of n .

Having established the reading process, we now set to describe how to write quantum information on this system. It would seem the best way to excite the system is

via a resonant ac current of frequency ω_5 in the external wires that, according to the Hamiltonian (18), will pump the beams to their excited state. However, such a current will also pump the beams to even higher excited states, since the energy level difference is fixed in this system. A better method would be to use constant currents in the external wires. The addition to the potential (4) due to such currents, keeping only first-order terms in B_1/B and B_2/B , is

$$H_1 = \frac{\pi E_J l_1}{I_c \beta_L \Phi_0} \{-B_1 x_1 [4I_c(\bar{\phi} - \phi_e) + I_b \beta_L] + B_2 x_2 [I_b \beta_L - 4I_c(\bar{\phi} - \phi_e)]\} \quad (24)$$

where constant terms were omitted and only linear terms in x_i were kept, owing to the quadratic terms being smaller by several orders of magnitude.

Since reading can be done only for the even mode, and the Hamiltonian (18) is separable into odd and even components, we do not consider the odd part in Eq. (24), and by choosing also $B_1 = B_2$, the even part of Eq. (24) is

$$H_{1,e} = -4\sqrt{2}\pi \frac{E_J l_1 \lambda_3 (\bar{\phi} - \phi_e)}{\beta_L \Phi_0} B_1 (a_5 + a_5^\dagger) \equiv f(B_1)(a_5 + a_5^\dagger), \quad (25)$$

where constant terms were again omitted. The even part of the total Hamiltonian $H + H_1$ is therefore

$$H_e = \hbar\omega_5 a_5^\dagger a_5 + f(B_1)(a_5 + a_5^\dagger). \quad (26)$$

The idea of writing is then the following: We create a constant magnetic field B_1 , which shifts the harmonic potential and then let the system relax to its new ground state. We then suddenly revert B_1 to zero thereby obtaining an excited state of the original system. The Hamiltonian in the differential representation is

$$H_e = -\frac{\hbar^2}{2m_1} \frac{d^2}{dx^2} + \frac{1}{2} m_1 \omega_5^2 x^2 + \lambda_3^{-1} f(B_1) x, \quad (27)$$

where the mass m_1 is the beam mass. Apart from a constant, the Hamiltonian (27) is

$$H_e = -\frac{\hbar^2}{2m_1} \frac{d^2}{dx^2} + \frac{1}{2} m_1 \omega_5^2 (x + \Delta x)^2, \quad (28)$$

$$\Delta x = \frac{f(B_1)}{m_1 \lambda_3 \omega_5^2}. \quad (29)$$

According to the scheme described above, we wish to maximize the probability $P_{nn} = |\langle\psi_0(x + \Delta x)|\psi_n(x)\rangle|^2$, with $\psi_n(x)$ being the n th harmonic oscillator wavefunction, to obtain the desired state $|n\rangle$ by tuning B_1 and with it Δx . Using standard results of the quantum harmonic oscillator to write the integral $\langle\psi_0(x + \Delta x)|\psi_n(x)\rangle$ and then using the generating function of the Hermite polynomials to find its value for every n , we find the maximum value of P_{nn} is reached when $\Delta x = 2\sqrt{n}\lambda_3$

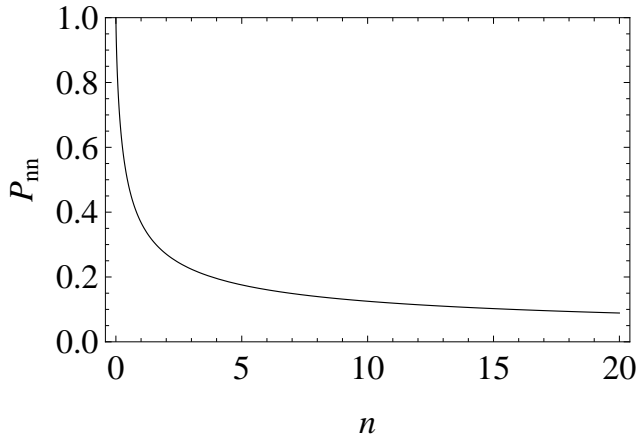


FIG. 2. Graph of the maximum probability of the ground state of the shifted harmonic potential having a $|n\rangle$ component in the unshifted potential. We have $P_{00} = 1$ and $P_{11} = e^{-1}$. The values for non-integer n were interpolated by $n! = \Gamma(n + 1)$.

with the probability then to measure k phonons after B_1 is removed given by

$$P_{kn} = (k!)^{-1} e^{-n} n^k, \quad (30)$$

which is a Poisson distribution with mean n . The P_{nn} function is plotted in Fig. 2. We see that the probability drops sharply for small n and evens out for larger values. The limit at $n \rightarrow \infty$ is 0. Although the writing process does not create a pure number state $|n\rangle$, the standard deviation in the number of phonons, by the properties of the Poisson distribution, is \sqrt{n} , which is reasonably low.

IV. SQUEEZED STATES

Having shown how to read and write quantum information in this system, we now wish to demonstrate the possibility of creating squeezed states. In an effort to mimic the Hamiltonian of a degenerate parametric amplifier from quantum optics³², we set the external wires magnetic fields to oscillate at double the frequency of the even mode, namely,

$$\begin{aligned} B_1 &= B_{1,0} e^{2i\langle\omega_5\rangle t} + \text{c.c.}, \\ B_2 &= B_{2,0} e^{2i\langle\omega_5\rangle t} + \text{c.c.}, \end{aligned} \quad (31)$$

where $\langle\omega_5\rangle$ denotes the time average of ω_5 , and the oscillations of ω_5 about this average are small since $B_i \ll B$.

The non-interacting Hamiltonian is found from Eq. (18) to be

$$H_0 = \hbar\langle\omega_5\rangle a_5^\dagger a_5 + \hbar\langle\omega_6\rangle a_6^\dagger a_6. \quad (32)$$

Keeping only terms to first order in B_i/B , the addition to the potential (4) due to the oscillating magnetic field in the rotating wave approximation (RWA), valid here due to the weak damping, is

$$H_I = \frac{4\pi E_J l_1^2 B}{\Phi_0^2 \beta_L} \{(B_1 + B_2)x_1 x_2 + B_1 x_1^2 + B_2 x_2^2\}. \quad (33)$$

We write this addition in terms of ladder operators, take $B_{1,0} = B_{2,0}$ to be pure imaginary and eliminate constant terms to find the interaction picture Hamiltonian in the RWA to be

$$H_I = \frac{8\pi i \langle\lambda_3\rangle^2 E_J l_1^2 B |B_{1,0}|}{\Phi_0^2 \beta_L} \{a_5^2 - (a_5^\dagger)^2\}, \quad (34)$$

which is the squeezing Hamiltonian. In writing Eq. (34) we neglected the time-dependent term $(\omega_5 - \langle\omega_5\rangle) a_5^\dagger a_5 + (\omega_6 - \langle\omega_6\rangle) a_6^\dagger a_6$, since it is negligible relative to the squeezing term under the assumed experimental conditions. It is interesting to note that squeezing of the odd mode is not possible using this scheme, even if ω_5 is replaced with ω_6 in Eq. (31). The fundamental reason for this is Lenz law, which makes the coefficient of $x_1 x_2$ in Eq. (33) positive and thus excludes terms proportional to a_6^2 in Eq. (34). The coefficient is positive because moving both beams in the positive direction costs energy, since both movements decrease the magnetic flux.

We now consider the effect of squeezing in this system and devise means to observe it. We assume dissipation is weak, and both beams are initially in the ground state. Conforming to standard notation, the squeezing parameter is

$$g = \frac{16\pi \langle\lambda_3\rangle^2 E_J l_1^2 B |B_{1,0}| t}{\hbar \Phi_0^2 \beta_L}, \quad (35)$$

which is real, and the squeezing operator reads

$$S(g) = \exp[g(a_5^2 - (a_5^\dagger)^2)/2]. \quad (36)$$

The time evolution of the a_5 operator in the interaction picture is given by

$$S^\dagger(g) a_5 S(g) = a_5 \cosh g - a_5^\dagger \sinh g. \quad (37)$$

In the rotating frame the uncertainty in the positions and momenta of the beams are

$$\langle\Delta x_i\rangle = \lambda_4 (1 + \tanh(g + \ln(\omega_5/\omega_6)/2))^{-1/2}, \quad (38)$$

$$\langle\Delta p_i\rangle = \frac{\hbar}{2} \lambda_4^{-1} (1 - \tanh(g + \ln(\omega_5/\omega_6)/2))^{-1/2}, \quad (39)$$

where Eqs. (7), (9), (15), (16) and (37) were used. We see that we have limited squeezing to below the standard quantum limit in the positions and unlimited anti-squeezing in the momenta, as the even mode is squeezed, while the odd mode is not. The interaction modifies the squeezing by adding the positive term of $\ln(\omega_5/\omega_6)/2$ to the squeezing parameter. In addition, with the product of the uncertainties being

$$\langle\Delta x_i\rangle \langle\Delta p_i\rangle = \frac{\hbar}{2} \cosh(g + \ln(\omega_5/\omega_6)/2), \quad (40)$$

we see that due to the interaction the minimum uncertainty is no longer attained before squeezing takes place.

It is interesting to write the wavefunction for the beams in the differential representation in the presence of squeezing. This wavefunction can be found by using the relation between the two-photon coherent states and the squeezed states³² to write for the squeezed state $|g\rangle$

$$(\cosh ga_5 + \sinh ga_5^\dagger)a_6|g\rangle = 0. \quad (41)$$

After moving to the differential representation, Eq. (41) is solved to find a wavefunction of the form

$$\psi(x_e, x_o) = C_1 e^{-\frac{m_1 \omega_5}{2\hbar} e^{2g} x_e^2} e^{-\frac{m_1 \omega_6}{2\hbar} x_o^2}, \quad (42)$$

with C_1 being a normalizing constant. When we transform this wavefunction to the beam coordinates via Eq. (14) we find that the new wavefunction is in a jointly Gaussian form, namely

$$\psi(x_1, x_2) = C_1 \exp\left(-\frac{\frac{x_1^2}{\sigma_1^2} + \frac{x_2^2}{\sigma_2^2} - \frac{2rx_1x_2}{\sigma_1\sigma_2}}{2(1-r^2)}\right), \quad (43)$$

where $\sigma_1 = \sigma_2 = \sqrt{2}\langle\Delta x_1\rangle$, with $\langle\Delta x_1\rangle$ given by Eq. (38), and the correlation coefficient given by

$$r = -\tanh(g + \ln(\omega_5/\omega_6)/2). \quad (44)$$

We note that the factor of $\sqrt{2}$ in σ_i comes from $|\psi(x_1, x_2)|^2$, rather than $\psi(x_1, x_2)$, being the probability distribution. In addition, we see that, as before, the beam interaction results in an addition to the squeezing parameter, which gives negative correlation even at $t = 0$. The correlation due to the squeezing is negative, because the influence of the odd mode, which is not squeezed, increases with time, producing perfect anti-correlation when the squeezing parameter goes to infinity.

Lastly, we consider the effect of the squeezing on the measurement of the magnetic flux in the SQUID. Using Eq. (22), we find the standard deviation of $\hat{\Phi}$ in the rotating frame to be

$$\langle\Delta\hat{\Phi}\rangle = \sqrt{2}(B + B_1)l_1\lambda_3 e^{-g}, \quad (45)$$

which is fully squeezed, while in the lab frame we have

$$\langle\Delta\hat{\Phi}\rangle = \sqrt{2}(B + B_1)l_1\lambda_3 \times \sqrt{\cosh(2g) - \sinh(2g) \cos(2\omega_5 t)}, \quad (46)$$

which characteristically oscillates between fully squeezed values at $t = (\pi/\omega_5)p$, corresponding to Eq. (45), and fully anti-squeezed values at $t = (\pi/\omega_5)(p + 1/2)$, where p is an integer. We conclude that the squeezing effect is measurable, and that the squeezing parameter can be found from the measurements.

V. EFFECT OF MECHANICAL DAMPING

In reality, the damping of the beam oscillations is weak but nonzero. With regard to reading and writing quantum information, this is not a problem, so long as the

reading or writing is performed within a period much shorter than the characteristic decay time. The squeezed states, however, are measurably degraded even by very weak dissipation, as we show in this section.

Many models were devised for describing dissipation in quantum systems⁴¹. We choose here to work with the quantum master equation. In the interaction picture with the Hamiltonian (34), the quantum master equation takes the form⁴²

$$\frac{\partial}{\partial t}\rho(t) = \mathcal{L}_S\rho(t) + \mathcal{L}_{dis}\rho(t), \quad (47)$$

$$\mathcal{L}_S\rho(t) = \frac{1}{2}\zeta[a^2 - (a^\dagger)^2, \rho(t)], \quad (48)$$

$$\begin{aligned} \mathcal{L}_{dis}\rho(t) = & -\frac{\gamma}{2}(n_{cav} + 1)\{[a^\dagger, a\rho(t)] + [\rho(t)a^\dagger, a]\} \\ & -\frac{\gamma}{2}n_{cav}\{[a, a^\dagger\rho(t)] + [\rho(t)a, a^\dagger]\}, \end{aligned} \quad (49)$$

where $\zeta = g/t$ is the squeezing rate and for brevity we write a instead of a_5 and ω instead of ω_5 . In Eqs. (47-49) $\rho(t)$ is the statistical operator for the system, \mathcal{L}_S and \mathcal{L}_{dis} are the Liouville operators for the squeezing and dissipation, respectively, $\gamma = \omega/Q$ is the damping rate of the even mode, where Q is the beam quality factor, and $n_{cav} = (e^{\hbar\omega/k_B T} - 1)^{-1}$ is the average phonon occupation in the even mode.

The system can be equivalently described by the Wigner quasi-probability distribution $W(\alpha, \alpha^*)$ instead of by the statistical operator $\rho(t)$, where we omit the explicit time dependence in $W(\alpha, \alpha^*)$ to make the notation concise. The parameter $\alpha = X_1 + iX_2$ is a complex number that is related to the phase space coordinates via $\alpha = \frac{1}{2\lambda}x + \frac{i\lambda}{\hbar}p$, where x and p are the even mode position and momentum coordinates, respectively, and $\lambda = \sqrt{\hbar/2m_1\omega}$ as before. We convert^{7,41} Eq. (47) to an equation for the Wigner distribution to find

$$\begin{aligned} \frac{\partial W(X_1, X_2)}{\partial t} = & [\zeta(X_1 \frac{\partial}{\partial X_1} - X_2 \frac{\partial}{\partial X_2}) + \frac{\gamma}{2}(\frac{\partial}{\partial X_1} X_1 + \frac{\partial}{\partial X_2} X_2) \\ & + \frac{1}{4}\gamma(n_{cav} + \frac{1}{2})(\frac{\partial^2}{\partial X_1^2} + \frac{\partial^2}{\partial X_2^2})]W(X_1, X_2), \end{aligned} \quad (50)$$

where we note that the original Wigner function $\overline{W}(x, p)$ is related to the one used here by $W(\alpha, \alpha^*) = W(X_1, X_2) = 2\hbar\overline{W}(x, p)$.

Equation (50) is seen to be a special case of the Fokker-Planck equation with $W(\mathbf{u})$ corresponding to the probability distribution $P(\mathbf{u}; t)$, where $\mathbf{u} = (X_1, X_2)$. Put in this form, the equation can be formally written as

$$\frac{\partial W(\mathbf{u})}{\partial t} = -\nabla \cdot [\mathbf{F}(\mathbf{u})W(\mathbf{u})] + \frac{D_0}{2}\nabla^2 W(\mathbf{u}), \quad (51)$$

where $\mathbf{F} = (-\zeta + \frac{\gamma}{2})X_1, (\zeta - \frac{\gamma}{2})X_2$ and $D_0 = \frac{1}{2}\gamma(n_{cav} + \frac{1}{2})$ are the force and diffusion constant, respectively. Due to the form of the force in Eq. (51), we can use separation of variables to break this equation into two one-dimensional Fokker-Planck equations with solutions $W_1(X_1)$ and $W_2(X_2)$, where $W(X_1, X_2) = W_1(X_1)W_2(X_2)$. These solutions are given by ($i = 1, 2$)

$$W_i(X_i) = \frac{1}{\sqrt{2\pi}\sigma_i(t)} \exp\left(-\frac{X_i^2}{2\sigma_i^2(t)}\right), \quad (52)$$

$$\sigma_i(t) = \sqrt{\left(\frac{1}{4} - \frac{D_0}{k_i}\right)e^{-k_i t} + \frac{D_0}{k_i}}, \quad (53)$$

$$k_1 = 2\zeta + \gamma, \quad (54)$$

$$k_2 = \gamma - 2\zeta, \quad (55)$$

where k_i are the decay rates.

Equations (52-55) indicate that a steady-state solution always exists for $W_1(X_1)$ and is given by Eq. (52) with $\sigma_1(t) = \sqrt{D_0/k_1}$. This finite distribution width corresponds to a saturation in the squeezing in contrast with the dissipationless case, when the field quadrature X_1 is squeezed without limit.³² For $W_2(X_2)$ on the other hand, we have a steady-state solution only at the strong damping regime, $\gamma > 2\zeta$, and this solution exhibits $\sigma_2(t) = \sqrt{D_0/k_2}$. When the strong damping condition is not satisfied, k_2 is negative, there is no steady state, and X_2 is anti-squeezed as in the dissipationless case³², but at a slower pace since the leading behavior in ΔX_2 is $e^{(\zeta-\gamma/2)t}$ instead of $e^{\zeta t}$ as in the dissipationless case.

The knowledge of the Wigner function in Eq. (52) enables us to calculate of system properties via the relation⁴¹

$$\langle \{a^r (a^\dagger)^s\}_{\text{sym}} \rangle = \int d^2\alpha \alpha^r (\alpha^*)^s W(\alpha, \alpha^*), \quad (56)$$

where $\{\cdot\}_{\text{sym}}$ indicates the average of all the permutations of the ladder operators, and $d^2\alpha = dX_1 dX_2$. Working in the rotating frame, the resulting uncertainties in the positions and momenta of the beams read ($i = 1, 2$)

$$\langle \Delta x_i \rangle = \sqrt{2}\lambda_3 \sqrt{\frac{1}{4} \frac{\omega_5}{\omega_6} + \sigma_1(t)^2}, \quad (57)$$

$$\langle \Delta p_i \rangle = \frac{1}{\sqrt{2}}\hbar\lambda_3^{-1} \sqrt{\frac{1}{4} \frac{\omega_6}{\omega_5} + \sigma_2(t)^2}, \quad (58)$$

which reduce to Eqs. (38-39) when $\gamma = 0$.

We see that the squeezing in the position coordinates, already limited to $\sqrt{\omega_3/2\omega_6}$ of the standard quantum limit, λ_1 , in the dissipationless case of Eq. (38), is limited here as well with the same limit, where we take $n_{\text{cav}} = 0$ due to the previous assumption of $\hbar\omega \gg k_B T$. The momenta uncertainties, in comparison, are anti-squeezed only in the weak damping regime, $\gamma < 2\zeta$, compared with being always anti-squeezed in Eq. (39), when there is no damping. As with the quadrature field X_2 , the momenta anti-squeezing in the weak damping regime has a slower rate relative to the dissipationless case with a leading behavior of $e^{(\zeta-\gamma/2)t}$ vs. $e^{\zeta t}$ for the dissipationless case. The product of the position and momentum uncertainties in Eqs. (57-58) gives the lowest uncertainty at $t = 0$ and higher values afterwards.

As in Sec. IV, we wish to find here the effect of squeezing on the measurement of the magnetic flux. Using Eq. (22), we find the standard deviation in the rotating frame to be

$$\langle \Delta \hat{\Phi} \rangle = 2\sqrt{2}(B + B_1)l_1\lambda_3\sigma_1(t), \quad (59)$$

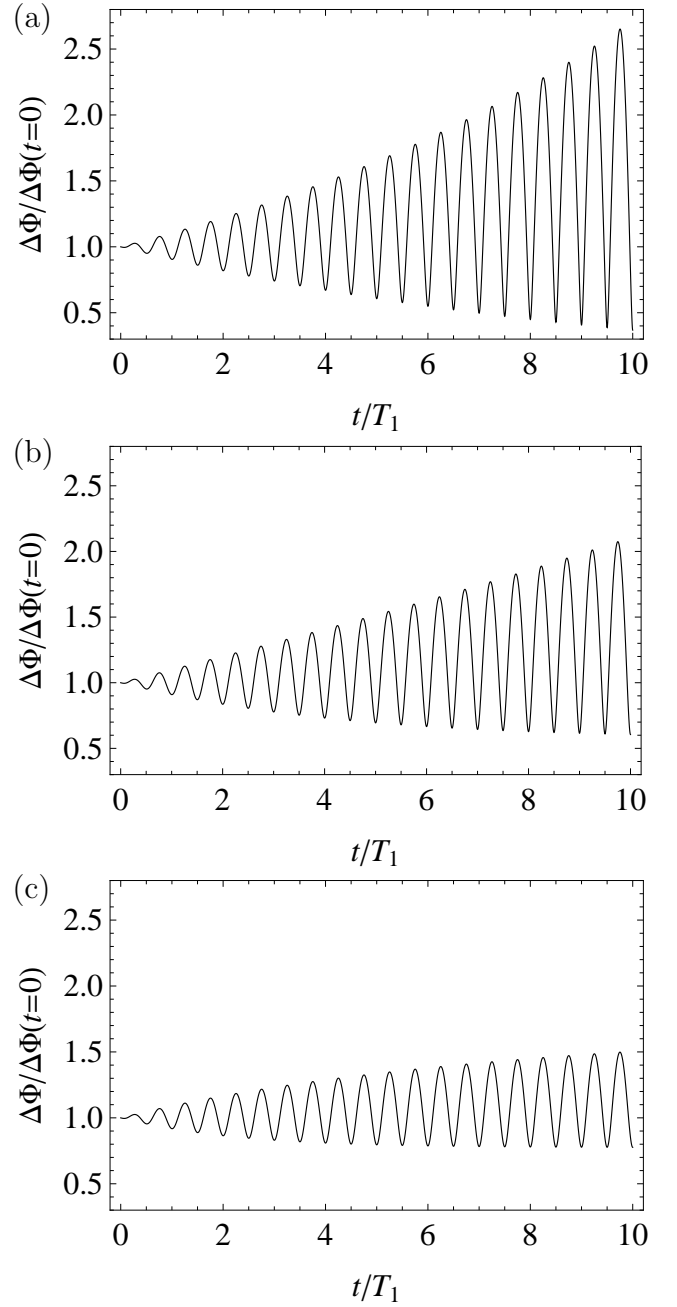


FIG. 3. Normalized deviation in the SQUID magnetic flux $\Delta\Phi(t)/\Delta\Phi(t=0)$ as a function of t/T_1 , where $n_{\text{cav}} = 0$, $T_1 = 2\pi/\omega$ and $\zeta = 0.1/T_1$. (a) No damping ($\gamma = 0$): Lower and upper limits are 0 and ∞ . (b) Weak damping ($\gamma = \zeta$): Lower and upper limits are $1/\sqrt{3}$ and ∞ . (c) Strong damping ($\gamma = 3\zeta$): Lower and upper limits are $\sqrt{3}/2$ and $\sqrt{3}$.

which is squeezed, though only to a finite extent unlike the dissipationless case in Eq. (45), where it is fully squeezed. In the lab frame we have

$$\langle \Delta \hat{\Phi} \rangle = 2\sqrt{2}(B + B_1)l_1\lambda_3 \times \sqrt{\cos^2(\omega t)\sigma_1^2(t) + \sin^2(\omega t)\sigma_2^2(t)}, \quad (60)$$

which oscillates between squeezed values at $t = (\pi/\omega)p$, corresponding to Eq. (59), and squeezed/anti-squeezed values, depending on the damping regime, at $t = (\pi/\omega)(p + 1/2)$, where p is an integer. In the dissipationless limit of $\gamma = 0$ Eq. (60) reduces to Eq. (46). Eq. (60) is plotted in Fig. 3 with normalized units for the no-damping, weak-damping and strong-damping cases. We conclude again that the squeezing effect is detectible and leads to reduced variation in the measured magnetic flux in the SQUID.

VI. CONCLUSIONS

In this work we have demonstrated that a system composed of two nanomechanical resonators embedded in a dc SQUID can be used as two units of quantum memory and that only the even mode in these two units is readable by the SQUID. We showed how the state of the beams can be altered, corresponding to writing quantum information, and proved the amplitude distribution of the number states in the resulting state is Poisson distributed. We then proposed a scheme to squeeze the even mode of the resonators and thus decrease the noise in the SQUID magnetic flux. Taking dissipation into account, we found a criterion that separates the weak damping regime, where a steady state exists only in one field quadrature, from the strong damping one, where both field quadratures exhibit steady states. We then predicted the form of the fluctuations in the magnetic flux in the SQUID, by which squeezing can be observed.

The approximations and assumptions made during our derivations hold well for reasonable experimental values. For instance, for two identical 8 MHz resonators of length $25 \mu\text{m}$ and quality factor $Q = 2 \cdot 10^4$, an external magnetic field of 10 T, beam temperature of 0.1 mK, SQUID temperature of 20 mK and other parameter values similar to the ones in Refs. 27 and 28, we find the energy level differences in the Hamiltonian (18) to be much larger than both $k_B T$ and the level widths. Moreover, for the reading process, Eq. (23) gives a required SQUID sensitivity of

$1.3 \cdot 10^{-5} \frac{\Phi_0}{\sqrt{\text{Hz}}}$ for $n \sim 1$ and sensitivity of $1.3 \cdot 10^{-5} \frac{1}{\sqrt{2n}} \frac{\Phi_0}{\sqrt{\text{Hz}}}$ for $n \gg 1$. A typical SQUID with a flux sensitivity of $10^{-6} \Phi_0/\sqrt{\text{Hz}}$ satisfies these conditions for $n < 80$.

Regarding the squeezing, a major question is whether substantial squeezing can be achieved within the decoherence time for the states. The decoherence time for the resonators here can be made to be at least $5 \mu\text{s}$ ^{19,43,44}, while substituting the parameters above in Eq. (35) gives a characteristic squeezing time of $\tau_{sq} \sim 2 \mu\text{s}$. We therefore conclude that substantial squeezing is achievable within the dephasing time.

The experimental realization of this system will be an important demonstration of macroscopic quantum behavior and squeezing in a nanomechanical system. In addition it can be used for detecting the position of the embedded nanomechanical beams with accuracy higher than the standard quantum limit. Stacking such SQUIDS in series, with the upper arm of the lower SQUID being also the lower arm of the upper one, can form a quantum data bus^{45,46}, lead to a multi-mode entangled state⁴⁷, and possibly multi-mode squeezing³². Another application of this system or a close variant of it is that of a quantum gate⁴⁷ acting on the two states by means of currents in the external wires. A series of such quantum gates can form the basis of a nanomechanical quantum computer^{48,49}. We leave the development of these ideas for future studies.

ACKNOWLEDGMENTS

This work has been partially funded by the NSF grant No. DMR-0802830. One of us (MD) is grateful to the Scuola Normale Superiore of Pisa for the hospitality during a visit where part of this work has been initiated, and to S. Pugnetti and R. Fazio for useful discussions.

REFERENCES

-
- * gcohen@physics.ucsd.edu
 - † diventra@physics.ucsd.edu
 - ¹ M. P. Blencowe, *Contemporary Phys.* **46:4**, 249 (2005).
 - ² K. Schwab and M. Roukes, *Phys. Today* **58**, 36 (2005).
 - ³ A. J. Leggett, "The lesson of quantum theory: Niels bohr centenary symposium," (Elsevier, Amsterdam, 1986) Chap. Quantum mechanics at the macroscopic level, pp. 35–58.
 - ⁴ A. J. Leggett, *J. Phys.: Condens. Matt.* **14**, R415 (2002).
 - ⁵ M. D. LaHaye, O. Buu, B. Camarota, and K. C. Schwab, *Science* **304**, 74 (2004).
 - ⁶ A. D. O'Connell, M. Hofheinz, M. Ansmann, R. C. Bialczak, M. Lenander, E. Lucero, M. Neeley, D. Sank, H. Wang, M. Weides, J. Wenner, J. M. Martinis, and A. N. Cleland, *Nature* **464**, 697 (2010).
 - ⁷ P. Rabl, A. Shnirman, and P. Zoller, *Phys. Rev. B* **70**, 205304 (2004).
 - ⁸ R. Ruskov, K. Schwab, and A. N. Korotkov, *Phys. Rev. B* **71**, 235407 (2005).
 - ⁹ X. Zhou and A. Mizel, *Phys. Rev. Lett.* **97**, 267201 (2006).
 - ¹⁰ C. Li and T.-W. Chou, *Appl. Phys. Lett.* **84:25**, 5246 (2004).
 - ¹¹ E. Buks and B. Yurke, *Phys. Rev. E* **74**, 046619 (2006).
 - ¹² K. Jensen, K. Kim, and A. Zettl, *Nature Nanotech.* **3**, 533 (2008).
 - ¹³ M. P. Blencowe and E. Buks, *Phys. Rev. B* **76**, 014511 (2007).

- ¹⁴ C. Stampfer, A. Jungen, R. Linderman, D. Obergfell, S. Roth, and C. Hierold, *Nano Lett.* **6**, 1449 (2006).
- ¹⁵ R. H. Blick, A. Erbe, H. Krömmel, A. Kraus, and J. P. Kotthaus, *Physica E* **6**, 821 (2000).
- ¹⁶ R. H. Blick, H. Qin, H.-S. Kim, and R. Marsland, *New Jour. Phys.* **9**, 241 (2007).
- ¹⁷ I. Mahboob and H. Yamaguchi, *Nature Nanotech.* **3**, 275 (2008).
- ¹⁸ A. Schliesser, O. Arcizet, R. Rivière, G. Anetsberger, and T. J. Kippenberg, *Nature Phys.* **5**, 509 (2009).
- ¹⁹ C. A. Regal, J. D. Teufel, and K. W. Lehnert, *Nature Phys.* **4**, 555 (2008).
- ²⁰ X. M. H. Huang, J. Hone, C. A. Zorman, and M. Mehregany, *IEEE Sens. J.* **30**, 1042 (2005).
- ²¹ D. Mozyrsky, I. Martin, and M. B. Hastings, *Phys. Rev. Lett.* **92**, 018303 (2004).
- ²² E. K. Irish and K. Schwab, *Phys. Rev. B* **68**, 155311 (2003).
- ²³ J. Suh, M. D. LaHaye, P. M. Echternach, K. C. Schwab, and M. L. Roukes, *Nano Lett.* **10**, 3990 (2010).
- ²⁴ F. Xue, Y. D. Wang, C. P. Sun, H. Okamoto, H. Yamaguchi, and K. Semba, *New Jour. Phys.* **9**, 35 (2007).
- ²⁵ L. L. Benatov and M. P. Blencowe, *Phys. Rev. B* **86**, 075313 (2012).
- ²⁶ N. Lambert and F. Nori, *Phys. Rev. B* **78**, 214302 (2008).
- ²⁷ S. Etaki, M. Poot, I. Mahboob, K. Onomitsu, H. Yamaguchi, and H. S. J. Van Der Zant, *Nature Phys.* **4**, 785 (2008).
- ²⁸ M. Poot, S. Etaki, I. Mahboob, K. Onomitsu, H. Yamaguchi, Y. M. Blanter, and H. S. J. van der Zant, *Phys. Rev. Lett.* **105**, 207203 (2010).
- ²⁹ E. Buks and M. P. Blencowe, *Phys. Rev. B* **74**, 174504 (2006).
- ³⁰ E. Buks, E. Segev, S. Zaitsev, B. Abdo, and M. P. Blencowe, *Eur. Phys. Lett.* **81**, 10001 (2008).
- ³¹ D. F. Walls, *Nature* **306**, 141 (1983).
- ³² D. F. Walls and G. J. Milburn, *Quantum Optics*, 2nd ed. (Springer, 2008).
- ³³ J. D. Teufel, T. Donner, M. A. Castellanos-Beltran, J. W. Harlow, and K. W. Lehnert, *Nature Nanotech. Lett.* **4**, 820 (2009).
- ³⁴ F. Xue, Y.-X. Liu, C. P. Sun, and F. Nori, *Phys. Rev. B* **76**, 064305 (2007).
- ³⁵ S. Pugno, Y. M. Blanter, and R. Fazio, *Eur. Phys. Lett.* **90**, 48007 (2010).
- ³⁶ C. P. Poole Jr., H. A. Farach, R. J. Creswick, and R. Prozorov, *Superconductivity*, 2nd ed. (Academic Press, 2007).
- ³⁷ J. S. Aldridge and A. N. Cleland, *Phys. Rev. Lett.* **94**, 156403 (2005).
- ³⁸ G. Z. Cohen, Y. V. Pershin, and M. Di Ventra, *Phys. Rev. B* **85**, 165428 (2012).
- ³⁹ J. D. Teufel, C. A. Regal, and K. W. Lehnert, *New Jour. Phys.* **10**, 095002 (2008).
- ⁴⁰ H. Bruus and K. Flensberg, *Many-Body Quantum Theory in Condensed Matter Physics: An Introduction* (Oxford University Press, 2004).
- ⁴¹ C. W. Gardiner and P. Zoller, *Quantum Noise*, 3rd ed. (Springer, 2004).
- ⁴² R. Y. Chiao and J. C. Garrison, *Quantum Optics*, 1st ed. (Oxford, 2008).
- ⁴³ S. Gröblacher, K. Hammerer, M. R. Vanner, and M. Aspelmeyer, *Nature* **460**, 724 (2009).
- ⁴⁴ E. Verhagen, S. Deléglise, S. Weis, A. Schliesser, and T. J. Kippenberg, *Nature* **482**, 63 (2012).
- ⁴⁵ Y. Li, T. Shi, B. Chen, Z. Song, and C.-P. Sun, *Phys. Rev. A* **71**, 022301 (2005).
- ⁴⁶ M. A. Sillanpää, J. I. Park, and R. W. Simmonds, *Nature* **449**, 438 (2007).
- ⁴⁷ M. A. Nielsen and I. L. Chuang, *Quantum Computation and Quantum Information*, 1st ed. (Cambridge University Press, 2000).
- ⁴⁸ A. N. Cleland and M. R. Geller, *Phys. Rev. Lett.* **93**, 070501 (2004).
- ⁴⁹ T. D. Ladd, F. Jelezko, R. Laflamme, Y. Nakamura, C. Monroe, and J. L. O'Brien, *Nature* **464**, 45 (2010).